Essential role of PI3-kinase and phospholipase A2 in *Dictyostelium discoideum* chemotaxis

Peter J.M. van Haastert, Ineke Keizer-Gunnink, and Arjan Kortholt

Department of Molecular Cell Biology, University of Groningen, 9751NN Haren, the Netherlands

Chemotaxis toward different cyclic adenosine monophosphate (cAMP) concentrations was tested in *Dictyostelium discoideum* cell lines with deletion of specific genes together with drugs to inhibit one or all combinations of the second-messenger systems PI3-kinase, phospholipase C (PLC), phospholipase A2 (PLA2), and cytosolic Ca^{2+}. The results show that inhibition of either PI3-kinase or PLA2 inhibits chemotaxis in shallow cAMP gradients, whereas both enzymes must be inhibited to prevent chemotaxis in steep cAMP gradients, suggesting that PI3-kinase and PLA2 are two redundant mediators of chemotaxis. Mutant cells lacking PLC activity have normal chemotaxis; however, additional inhibition of PLA2 completely blocks chemotaxis, whereas inhibition of PI3-kinase has no effect, suggesting that all chemotaxis in *plc*-null cells is mediated by PLA2. Cells with deletion of the IP_3 receptor have the opposite phenotype: chemotaxis is completely dependent on PI3-kinase and insensitive to PLA2 inhibitors. This suggest that PI3-kinase–mediated chemotaxis is regulated by PLC, probably through controlling PIP_2 levels and phosphatase and tensin homologue (PTEN) activity, whereas chemotaxis mediated by PLA2 appears to be controlled by intracellular Ca^{2+}.

Introduction

Chemotaxis is a pivotal response of many cell types to external spatial cues. It plays important roles in diverse functions, such as finding nutrients in prokaryotes, forming multicellular structures in protozoa, tracking bacterial infections in neutrophils, and organizing the embryonic cells in metazoa (Baggiolini, 1998; Campbell and Butcher, 2000; Crone and Lee, 2002). In *Dictyostelium discoideum* cells, extracellular cAMP functions as a chemoattractant that is detected by specific G protein–coupled surface receptors. Chemotaxis is achieved by coupling gradient sensing to basic cell movement. Two important questions on chemotaxis are (1) What is the compass detecting the cAMP gradient? and (2) How is this signal transduced to localized pseudopod formation?

Pseudopod extension at the leading edge is mediated by the formation of new actin filaments, whereas acto-myosin filaments in the rear of the cell inhibit pseudopod formation and retract the uropod. In *D. discoideum*, myosin filament formation is regulated by cGMP (Bosgraaf and van Haastert, 2006), whereas in mammalian cells it is regulated by Rho-kinases (Xu et al., 2003). We are beginning to understand the signals that regulate actin polymerization at the front of the cell (Van Haastert and Devreotes, 2004; Affolter and Weijer, 2005; Franca-Koh et al., 2007). Phosphatidylinositol (3,4,5)-trisphosphate (PIP_3) is a very strong candidate to mediate directional sensing in neutrophils and *D. discoideum*. PIP_3 is formed at the side of the cell closest to the source of chemoattractant (Parent et al., 1998; Hirsch et al., 2000; Servant et al., 2000; Funamoto et al., 2002; Iijima and Devreotes, 2002). Furthermore, PIP_3 is a very strong inducer of pseudopod extensions, as demonstrated in *pten* (*phosphatase and tensin homologue*)–null mutants with elevated PIP_3 levels, and subsequently more pseudopods (Iijima and Devreotes, 2002). Unexpectedly, inhibition of PI3-kinase (PI3K) has only moderate effects on chemotaxis in *D. discoideum* (Funamoto et al., 2002; Iijima and Devreotes, 2002; Postma et al., 2004b; Loovers et al., 2006) and mammalian cells (Wang et al., 2002; Ward, 2004, 2006), demonstrating that PI3K signaling is dispensable for chemotaxis.

What are the signaling pathways that mediate chemotaxis in *pi3k*-null cells? It has been argued that the optimal second messenger mediating directional sensing will have a lifetime of ~5 s and a diffusion rate constant of ~1 $\mu m^2/s$ (Postma et al., 2004a). Molecules like cAMP, cGMP, H^+, K^+, or IP_3 do not meet these criteria. PIP_3, however, perfectly fits in this biophysical profile: very low basal levels, rapid transient accumulation after cAMP

Correspondence to Peter J.M. van Haastert: P.J.M.van.Haastert@rug.nl

Abbreviations used in this paper: BPB, p-bromophenacyl bromide; PI3K, PI3-kinase; PIP_2, phosphatidylinositol (4,5)-bisphosphate; PIP_3, phosphatidylinositol (3,4,5)-trisphosphate; PTEN, phosphatase and tensin homologue.

The online version of this article contains supplemental material.

The Journal of Cell Biology, Vol. 177, No. 5, June 04, 2007 809–816
http://www.jcb.org/cgi/doi/10.1083/jcb.200701134

stimulation with a half-life of ~5 s, and a diffusion rate constant of ~0.5 $\mu m^2/s$ (Postma et al., 2004a). Possible alternatives for PIP_3 in *pi3k*-null cells are the lipid products of PLC, PLA2, and PLD, or combinations of these enzymes. Ca^{2+} may play a role in chemotaxis as well, because in cells its diffusion is rather slow (Tsaneva-Atanasova et al., 2005). In this study, we investigated the role of several potential second-messenger systems in *D. discoideum* chemotaxis. The results show that inhibition of PI3K and PLA2 strongly reduces chemotaxis. Inhibition of PLC or intracellular Ca^{2+} signaling has little direct effect on chemotaxis. However, chemotaxis in *plc*-null cells appears to be completely dependent on PLA2 activity, whereas chemotaxis in cells lacking the IP_3 receptor depends only on PI3K activity, suggesting that PLC and intracellular Ca^{2+} are not mediators of chemotaxis but regulate the activity of PI3K and PLA2, respectively.

Results

The chemoattractant cAMP stimulates at least eight second-messenger systems in *D. discoideum*, adenylyl cyclases, guanylyl cyclases, proton production, K^+ fluxes, Ca^{2+} uptake and release from internal stores, PLC, PI3K, and PLA2. Null mutants of most second-messenger systems have been made; none of these mutants exhibit a severe chemotactic defect (Van Haastert and Devreotes, 2004; Affolter and Weijer, 2005). Apparently, multiple pathways mediate chemotaxis. To identify the signaling pathways that collectively mediate chemotaxis, we measured chemotaxis in several mutant cells treated with mixtures of drugs to inhibit one, multiple, or all messenger systems. To limit the number of combinations to be tested (all possible combinations of 8 pathways is 8! or 40,320 conditions), as explained in the Introduction, we identified potential second messengers that have a diffusion rate constant between 0.3 and 3 $\mu m^2/s$ and accumulate transiently with a lifetime of 3–10 s after stimulation with the chemoattractant cAMP. Potential second messengers are phospholipids such as PIP_3 and phosphatidylinositol (4,5)-bisphosphate (PIP_2), fatty acids, and cytosolic Ca^{2+}. Therefore, we investigated four signaling pathways, PI3K, PLC, PLA2, and cytosolic Ca^{2+}.

For each second-messenger system, we aimed at collecting two independent datasets, obtained either with a mutant defective in that second-messenger system or with a drug inhibiting the enzyme activity, respectively. We have tested the following conditions: (1) *pi3k*-null or wild-type cells treated with the PI3K inhibitor LY294002 at a concentration of 50 μM, (2) *plc*-null or wild-type cells treated with the PLC inhibitor U73122 at a concentration of 10 μM, (3) the PLA2 inhibitors quinacrine at 20 μM and p-bromophenacyl bromide (BPB) at 2 μM, and (4) a combination of mutants and drugs to affect cytosolic Ca^{2+}, notably mutant cells lacking the IP_3 receptor in combination with 10 mM EGTA to block Ca^{2+} uptake. The concentrations of drugs used were obtained either from published dose response curves (U73122 [Seastone et al., 1999] and LY294002 [Loovers et al., 2006]) or from dose response curves presented in Fig. 1 for BPB and quinacrine. Half-maximal inhibition of chemotaxis to 50 nM cAMP was observed at 0.5 μM BPB or 5 μM quinacrine and >80% inhibition at a concentration of 2 μM BPB or

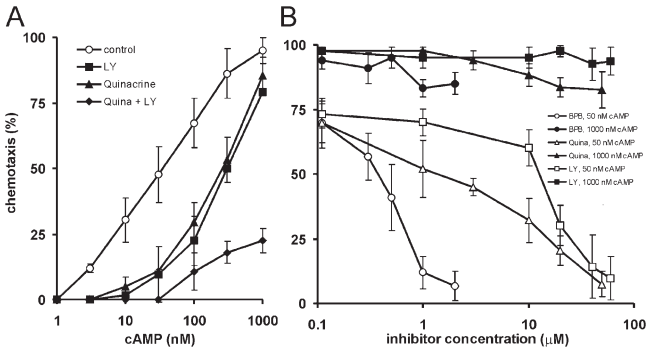

Figure 1. **Inhibition of chemotaxis by the PLA2 inhibitors BPB and quinacrine and the PI3K inhibitor LY294002.** Chemotaxis of wild-type cells was measured toward different concentrations of cAMP (A; with 50 μM LY294002, 20 μM quinacrine, and 2 μM BPB) at different concentrations of BPB, quinacrine, and LY294002 (B; with 50 and 1,000 nM cAMP). The results show strong inhibition at low cAMP concentrations but no inhibition at high cAMP concentrations.

50 μM quinacrine. Chemotaxis to 1,000 nM cAMP is only slightly inhibited, even at the highest concentrations used, indicating that BPB and quinacrine are not harmful to the cells. In addition, cells treated with BPB exhibit a normal PIP_3 response, as shown by the translocation of PHcrac-GFP to the leading edge, suggesting that inhibition of the PLA2 pathway does not interfere with the PI3K pathway (see Fig. 5 D).

All single and multiple combinations inhibiting four signaling pathways yielded ~70 experimental conditions, to be tested at two cAMP concentrations with at least three replicates (Table S1, available at http://www.jcb.org/cgi/content/full/jcb.200701134/DC1). We have used the small population assay (Konijn, 1970) to screen these 500 conditions. In this assay, small droplets containing wild-type or mutant cells are deposited on hydrophobic agar. Cells can freely move within the boundary of the droplet but cannot move out of the droplet. Therefore, any directional movement of the cells leads to the accumulation of cells at the boundary of the small population, which is rapidly scored. In the shallow absolute gradient induced by 50 nM cAMP (dC/dx = 100 pM/μm), a weak chemotaxis response is observed in ~50–70% of the populations, whereas 1,000 nM cAMP induces a steep absolute gradient (dC/dx = 2,000 pM/μm) and a strong chemotaxis response in 90–100% of the populations. In videos that were analyzed for detailed cell movement, chemotaxis by 50 nM cAMP had the characteristics of a biased random walk with a chemotaxis index of ~0.5, whereas the response toward 1,000 nM cAMP exhibits the characteristics of directional movement with a chemotaxis index of ~0.85. With this assay it is possible to simultaneously test, in 1 d, 30 different conditions (mutant cells or drugs) at two cAMP concentrations, each with 12 populations that are observed at least four times. This large dataset is presented as Table S1. In Figs. 2 and 3, the results are discussed in a logical and reduced format.

PI3K and PLA2 are mediators of chemotaxis

The *pi3k*-null mutant has deletions of two genes encoding PI3K1 and PI3K2 that, together, mediate essentially all cAMP-stimulated

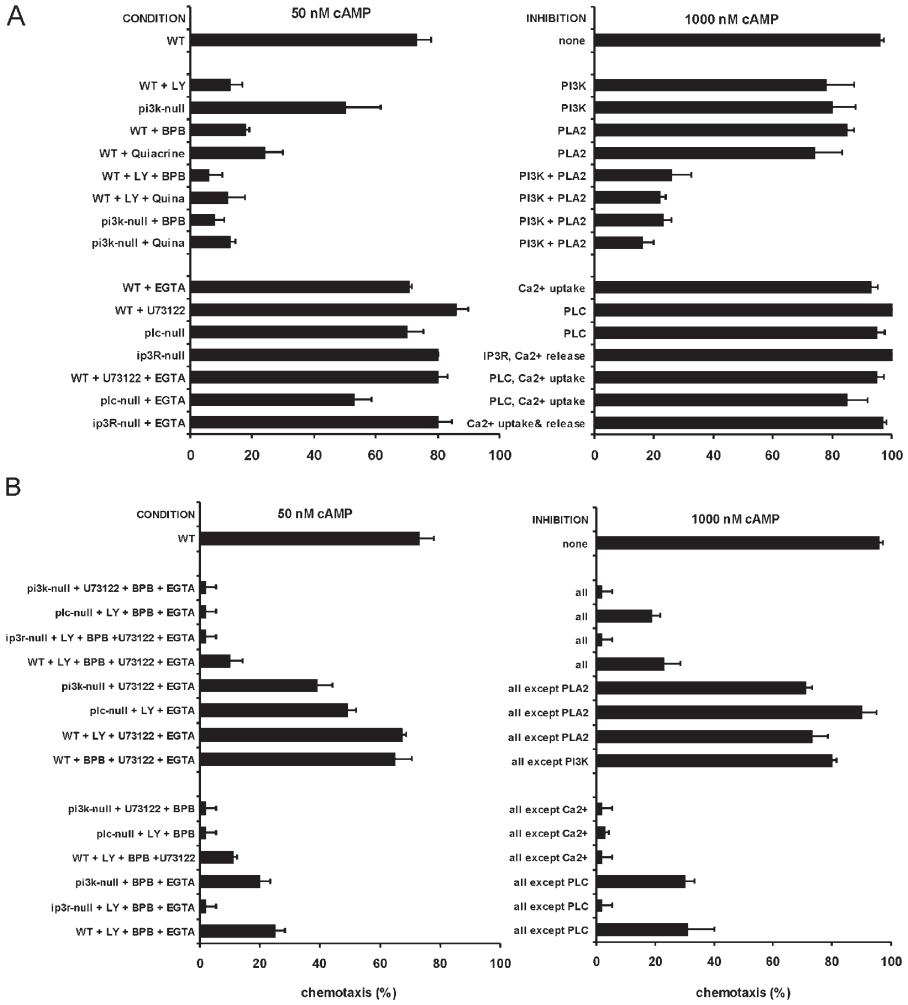

Figure 2. **Role of PI3K, PLA2, PLC, and cytosolic Ca^{2+} in *D. discoideum* chemotaxis.** Chemotaxis was measured in the absence or presence of 50 μM LY294002 (LY; PI3K inhibitor), 10 μM U73122 (PLC inhibitor), 20 μM quinacrine (Quina) and 2 μM BPB (PLA2 inhibitors), and 10 mM EGTA to block Ca^{2+} uptake. Four strains were used: wild-type (WT) AX3 and the mutants *pi3k*-null, *plc*-null, and the IP_3 receptor–null *iplA*$^-$ lacking the IP_3 receptor. Chemotaxis at 50 nM cAMP is a biased random walk, whereas chemotaxis at 1,000 nM exhibits directional movement. (A) Experiments are presented with increasing complexity of inhibitors, to find the second-messenger pathways that, together, are responsible for all chemotaxis. (B) Shown is a total mixture of inhibitors, leading to a complete blockade of chemotaxis, followed by decreasing complexity of inhibitors, to find the pathways that alone can induce chemotaxis. The results of A show that PI3K and PLA2 together are responsible for essentially all chemotaxis, and B shows that either the PI3K or the PLA2 pathway is sufficient to provide full chemotactic activity. The PLC and Ca^{2+} pathways apparently cannot mediate chemotaxis.

PIP_3 formation (Huang et al., 2003). Fig. 2 A reveals that inhibition of PI3K activity, either with LY294002 or by disruption of *pi3k*, results in reduced chemotactic activity when measured with 50 nM cAMP, but inhibition of PI3K has no effect at 1,000 nM cAMP. The 70% reduction of chemotaxis at 50 nM cAMP by LY294002 is substantially stronger that the 30% reduction seen in *pi3k1/2*-null cells. There are several potential explanations for this observation, such as the inhibition of the other PI3K3-5 by LY294002, the reduction of speed that is induced by LY294002 (Funamoto et al., 2002; Iijima and Devreotes, 2002; Loovers et al., 2006), or up-regulation of the PLA2 pathway in *pi3k*-null cells. The PLA2 inhibitors BPB and quinacrine have similar effects on chemotaxis as LY294002: partial inhibition at low cAMP concentrations but very little effect at high cAMP concentrations. When both PI3K and PLA2 enzyme activities are inhibited, nearly all chemotactic activity at both cAMP concentrations is lost.

A different strategy to identify the collective second-messenger systems for chemotaxis is presented in Fig. 2 B. First, all four second-messenger systems were blocked, by either a complete drug cocktail in wild-type cells (the PI3K inhibitor LY294002, the PLA2 inhibitors BPB or quinacrine, the PLC inhibitor U73122, and the Ca^{2+} inhibitor EGTA) or limited drug cocktails in mutants lacking *pi3k*, *plc*, or the IP_3 receptor gene *iplA*. In all these conditions, chemotaxis was completely blocked. Subsequently, one signaling pathway at a time was allowed to be active. The experiments reveal nearly normal chemotaxis when only PI3K or only PLA2 are active while the other three pathways are still inhibited (Fig. 2 B). The results of Fig. 2 indicate that PI3K or PLA2 alone can fully support chemotaxis and that both pathways must be inhibited to completely block chemotaxis.

The effect of inhibition of PI3K and PLA2 on chemotaxis was also investigated in an experimental setup where the cAMP gradient was created using micropipettes. Fig. 3 presents the analysis of a video (Video 1, available at http://www.jcb.org/cgi/content/full/jcb.200701134/DC1) in which cAMP-stimulated wild-type AX3 cells in buffer are treated sequentially with BPB and BPB + LY294002. The tracks of some representative cells are presented in Fig. 3 A, the chemotaxis index and speed of 30 cells for Video 1 in Fig. 3 B, and the mean of several videos in Fig. 3 C. A pipette with cAMP induces a strong chemotaxis response in buffer. Upon addition of BPB, chemotaxis continues with nearly the same chemotaxis index at a reduced speed. Similar observations were made previously with LY294002 in the absence of BPB, showing nearly normal chemotaxis when only PI3K is inhibited (Funamoto et al., 2002; Iijima and Devreotes, 2002;

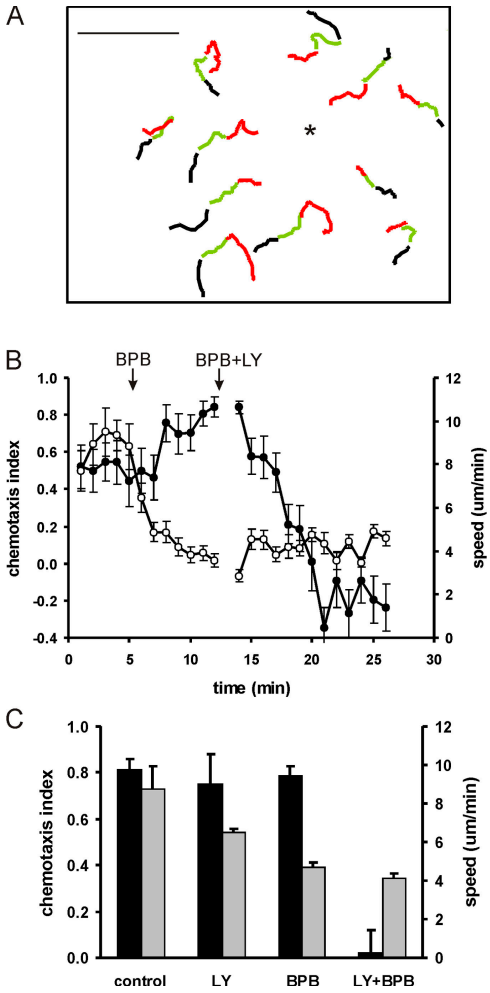

Figure 3. **Chemotaxis of wild-type AX3 cells measured with micropipettes.** A micropipette releasing cAMP is positioned in a field of cells at t = 0; at t = 4 min, 5 μM BPB is added, and at t = 12 min, 50 μM LY294002 is added. Images were captured every 10 s (presented as Video 1, available at http://www.jcb.org/cgi/content/full/jcb.200701134/DC1). (A) The tracks of 11 cells are shown for chemotaxis to a pipette with cAMP (asterisk) in buffer (black lines; t = 0–4 min) in BPB (green lines; t = 4–12 min) and LY294002 + BPB (red lines; t = 12–26 min). Bar, 100 μm. (B) The figure shows the chemotaxis index (closed circle) and speed (open circle) as means and SEM of ~30 cells. (C) The chemotaxis index (black bars) and speed (gray bars) of wild-type cells was determined in the absence or presence of 5 μM BPB and/or 50 μM LY294002. The data shown are the means and SEM of the chemotaxis index and speed from three independent experiments, each with ~30 cells, determined from 5 min after addition of the inhibitors.

Loovers et al., 2006; Fig. 3 C). However, upon addition of LY294002 to BPB-treated wild-type cells, chemotaxis toward the pipette is inhibited completely.

PLC and Ca^{2+} are not mediators of chemotaxis

Inhibition of PLC activity by deletion of the unique *plc* gene or with the inhibitor U73122 has no effect on chemotaxis (Fig. 2 A, bottom), consistent with previous experiments (Drayer et al., 1994). Interference with the cytosolic Ca^{2+} response, by either blocking Ca^{2+} uptake with EGTA or IP_3-mediated intracellular Ca^{2+} release in cells lacking the IP_3 receptor, also has no effect on chemotaxis at low or high cAMP concentrations. Fig. 2 B (bottom) presents the chemotactic data of conditions in which all pathways except PLC or Ca^{2+} are active, revealing that PLC or Ca^{2+} alone does not support chemotactic activity.

PLC and Ca^{2+} are regulators of chemotaxis

Although PLC and Ca^{2+} apparently cannot mediate chemotaxis, we have noticed that these second messengers appear to affect chemotaxis mediated by PI3K and PLA2. As shown above, chemotaxis of wild-type cells is partly inhibited by the PI3K inhibitor LY294002 and partly by the PLA2 inhibitors BPB or quinacrine. In contrast, chemotaxis of *plc*-null cells is not inhibited at all by the PI3K inhibitor LY294002 and is completely inhibited by the PLA2 inhibitor BPB (Fig. 4). This suggests that in *plc*-null cells, chemotaxis is mediated largely by PLA2 and not by PI3K. The mutant with a deletion of the IP_3 receptor has the opposite phenotype. Chemotaxis is indistinguishable from chemotaxis of wild type, as presented previously (Traynor et al., 2000), but now chemotaxis is completely blocked by the PI3K inhibitor LY294002, whereas the PLA2 inhibitors have no effect, suggesting that in IP_3 receptor–null cells, all chemotaxis is mediated by PI3K and not by PLA2. As shown in Fig. 2, inhibition of PLC activity or inhibition of Ca^{2+} response has little effect on chemotaxis. However, blockade of both PLC and all Ca^{2+} responses (IP_3 receptor null in EGTA treated with U73122) yield a very strong inhibition of chemotaxis at 50 and 1,000 nM cAMP, consistent with the prediction that, at this condition, both PI3K and PLA2 are inhibited.

Reduced PIP_3 response in *plc*-null cells

The notion that in *plc*-null cells all chemotaxis is apparently mediated by PLA2 and not by PI3K could imply that PI3K is not activated by cAMP in *plc*-null cells. To test this hypothesis, we transformed *plc*-null cells with the PIP_3 sensor PHcrac-GFP and stimulated the cells with cAMP. Wild-type cells that chemotax toward a pipette releasing cAMP exhibit a crescent of PHcrac-GFP at the leading edge (Parent et al., 1998). Such a crescent is still present in wild-type cells treated with the PLA2 inhibitor BPB but absent in wild-type cells treated with the PI3K inhibitor LY294002 (Fig. 5, C and D). Although *plc*-null cells exhibit very good chemotaxis toward a pipette with cAMP, PHcrac-GFP hardly localizes at the leading edge and remains cytosolic, as in unstimulated cells (Fig. 5 B). We conclude that *plc*-null cells show an impaired activation of the PI3K pathway, which explains why the PI3K inhibitor LY294002 has no effect on chemotaxis of *plc*-null cells and the PLA2 inhibitors show such a strong effect.

Discussion

Toward a model for chemotaxis in *D. discoideum*

The experiments reveal that PI3K and PLA2 signaling together are responsible for nearly all chemotaxis in shallow and steep cAMP gradients (Fig. 6). In steep cAMP gradients, both PI3K and PLA2 signaling must be inhibited to observe a reduction of chemotactic activity. However, in shallow gradients, inhibition of either one pathway already leads to a strong inhibition of

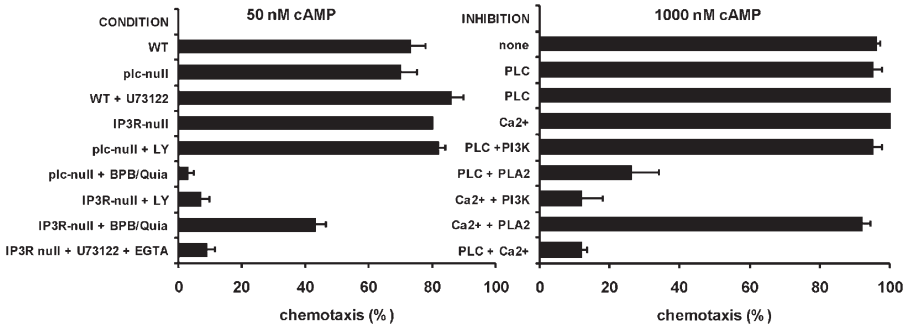

Figure 4. **PLC and Ca^{2+} are regulators of chemotaxis.** Chemotaxis was measured with the strains indicated in the absence or presence of the indicated inhibitors. The results show that inhibition of PLC or PLC and PI3K has little effect on chemotaxis, whereas inhibition of PLC and PLA2 completely blocks chemotaxis, suggesting that in *plc*-null cells, all chemotaxis is mediated by PLA2. Conversely, in IP_3 receptor–null cells, all chemotaxis is dependent on PI3K. Inhibition of both PLC and Ca^{2+} uptake and release in IP_3 receptor–null cells in EGTA and U73122 leads to complete inhibition of chemotaxis at both 50 and 1,000 nM cAMP. WT, wild type.

chemotaxis. Cell movement in buffer is best described as a random walk, i.e., every 30–60 s, cells extend a new pseudopod in a random direction. In shallow gradients, chemotaxis is essentially a biased random walk, i.e., new pseudopodia are still extended in all directions, but more frequently in the direction of the gradient than in other directions. We suppose that the time and place where a new pseudopod is made is regulated by activators and inhibitors and that stimulation of the cAMP receptor will influence the activity of one or multiple of these activators and inhibitors, thereby affecting pseudopod formation. In a shallow gradient, where the probability that a pseudopod is extended in the direction of the gradient is low, interference with any of these hypothetical activators or inhibitors will lead to a reduction of chemotaxis. The observation that in a shallow cAMP gradient, inhibition of either PI3K or PLA2 signaling inhibits chemotaxis suggests that downstream components of both pathways influence the probability of making a new pseudopod. In steeper gradients, nearly all pseudopodia are extended in the direction of the gradient, and interference with one of the hypothetical activators or inhibitors will have little effect as long as other activators or inhibitors remain functional. Thus, the PI3K and PLA2 pathways are both required for good chemotaxis in shallow gradients but are redundant in steep gradients.

The formation of second messengers at a specific place regulates the local formation of a pseudopod. These second messengers are presumably PIP_3 for the PI3K pathway, but there could be several second messengers for the PLA2 pathway. The PLA2-catalyzed hydrolysis of membrane phospholipids results in the stoichiometric production of a free fatty acid and a lysophospholipid. Both of these phospholipid metabolites may serve as potential second messengers. Recently, the first results of a genetic screen for LY294002-supersensitive chemotaxis mutants were reported (Chen et al., 2007). A gene was identified that belongs to the Ca^{2+}-independent PLA2 (iPLA2, group VI PLA2) class, whose inactivation in a wild-type background had no effect, but inactivation in a *pi3k*-null background nearly completely inhibited chemotaxis, which is in excellent agreement with the present observations. The regulation of this PLA2 by upstream components requires further investigation, as well as the identification of the messenger molecules of this PLA2 pathway that regulate pseudopod formation.

We routinely record chemotaxis data at a distance of 50–100 μm from the pipette, where that gradient is ~500–2,000 pM/μm. It should be mentioned that very close to the pipette, wild-type cells in LY294002 + BPB or *pi3k*-null cells in BPB exhibit a small but significant chemotaxis response ($P < 0.01$); the response was observed within 30 μm from the tip, where the gradient is very steep, at >12,500 pM/μm. This residual response close to the pipette is consistent with the small residual response in the small population assay in steep gradients toward 1,000 nM cAMP. We also observed that this residual response in LY294002 + BPB was somewhat stronger when cells are starved and pulsed with cAMP for 7, instead of 5, h. Several nonexclusive models may explain these observations, including residual PI3K and PLA2 activity resulting from partial inhibition of these enzymes, reduced uptake of the inhibitors in longer starved cells, or the presence of another signaling pathway that is active in very steep gradients or in cells starved for a longer period.

PLC and intracellular Ca^{2+} participate in chemotaxis, most likely not as mediators, but as regulators of PI3K and PLA2, respectively. Inhibition of the PLC and Ca^{2+} pathways in control cells has no effect on chemotaxis. However, significant chemotactic defects are observed when PLC or Ca^{2+} is inhibited in a background with inhibited PI3K or PLA2 ($P < 0.01$). The cAMP-mediated PIP_3 response is nearly absent in *plc*-null cells, and inhibitors suggest that chemotaxis in *plc*-null cells is exclusively mediated by PLA2. The mechanism by which *plc*-null

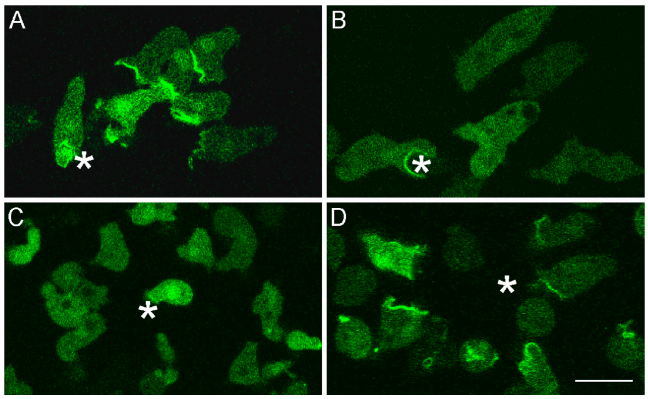

Figure 5. **Reduced PIP_3 formation in *plc*-null cells.** Wild-type cells (A, C, and D) and *plc*-null cells (B) expressing the PIP_3 sensor PHcrac-GFP were stimulated with a micropipette releasing a gradient of cAMP. Wild-type cells were incubated in buffer (A), 50 μM LY294002 (C), or 5 μM BPB (D). The results show a strongly diminished PIP_3 response in *plc*-null cells and wild-type cells treated with the PI3K inhibitor LY294002, but normal PIP_3 response of wild-type cells in buffer or treated with the PLA2 inhibitor BPB. The asterisks indicate the position of the pipette. Bar, 10 μm.

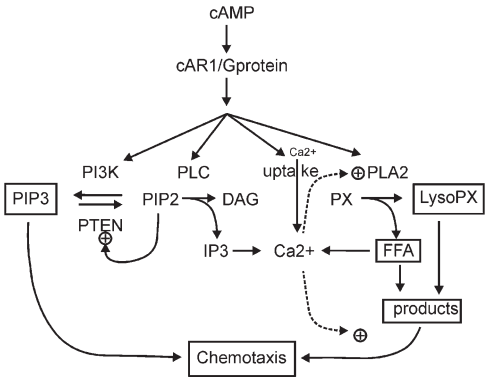

Figure 6. **Model of signaling cascades leading to *D. discoideum* chemotaxis.** cAMP activates multiple pathways. The PI3K and PLA2 pathway are parallel mediators of chemotaxis: either one can mediate chemotaxis, and chemotaxis is blocked nearly completely when both pathways are inhibited. PIP_3 is the likely mediator of the PI3K pathway, by recruiting PH-containing proteins modulating the actin cytoskeleton. The messenger of the PLA2 pathway controlling chemotaxis is unknown. The PI3K pathway appears to be controlled by the PLC pathway, presumably at the level of PIP_2 degradation, leading to a reduction of membrane-associated PTEN that degrades PIP_3. The PLA2 pathway is dependent on cytosolic Ca^{2+}, but it is unknown whether this occurs at the level of PLA2 activation or the action of downstream messengers on the chemotaxis system. Cytosolic Ca^{2+} is regulated by Ca^{2+} uptake from the medium (which is both G protein dependent and independent), free fatty acid (FFA)–mediated Ca^{2+} release from acidic stores, and the IP_3 receptor–mediated Ca^{2+} release from the endoplasmic reticulum.

cells have reduced PIP_3 levels is intriguing; *plc*-null cells have elevated PIP_2 levels (Drayer et al., 1994), i.e., more substrate for PI3K, which would predict increased PIP_3 levels, but we observed the opposite. It is known that the PIP_3-degrading enzyme PTEN binds to PIP_2, which is essential for its catalytic activity (Iijima et al., 2004), suggesting that the enhanced PIP_2 levels in *plc*-null cells trap PTEN at the membrane, preventing the accumulation of PIP_3. In accordance with this hypothesis, we observed that the level of membrane-associated PTEN-GFP is higher in *plc*-null cells than in wild-type cells (unpublished results), suggesting that the reduced PIP_3 level in *plc*-null cells is caused by enhanced activity of PTEN.

In *D. discoideum*, three pathways contribute to an elevation of cytosolic Ca^{2+} levels: (1) uptake of Ca^{2+} from the extracellular medium, (2) the IP_3 receptor–mediated release of Ca^{2+} from the endoplasmic reticulum, and (3) the fatty acid–mediated release of Ca^{2+} from acidosomes. The IP_3-mediated release of Ca^{2+} from internal stores cannot be inhibited by deleting the single *plc* gene, because in *D. discoideum*, IP_3 is also produced by degradation of IP_5, a pathway that is up-regulated in *plc*-null cells (Drayer et al., 1994; van Dijken et al., 1995). However, IP_3-mediated Ca^{2+} release can be effectively blocked by deletion of the IP_3 receptor in *iplA*-null cells (Traynor et al., 2000). Simultaneous inhibition of Ca^{2+} uptake and Ca^{2+} release pathways in *iplA*-null cells has little effect, but now chemotaxis is insensitive to PLA2 inhibitors and completely blocked by LY294002, indicating that chemotaxis is only mediated by the PI3K pathway. Apparently, the PLA2 pathway requires a rise in intracellular Ca^{2+}, which could be a direct effect of Ca^{2+} on the enzyme, as many PLA2 enzymes are Ca^{2+} dependent (Chakraborti, 2003).

In summary, we propose that chemotaxis at the leading edge of *D. discoideum* cells is mediated predominantly by two pathways, PI3K and PLA2 (Fig. 6). Each of these two pathways is regulated by another cAMP-stimulated pathway that, by itself, has no direct effect on chemotaxis. The PI3K pathway is regulated through PIP_2/PTEN by the PLC pathway. The PLA2 pathway depends on cytosolic Ca^{2+}, which is regulated by IP_3 (and thus partly by PLC), fatty acids (and thus partly by PLA2), and Ca^{2+} uptake. These intertwined and partly redundant signaling cascades make chemotaxis in *D. discoideum* very robust because multiple signaling pathways must be deleted to obtain a strong reduction of chemotaxis.

The model for chemotactic signaling may help focus experiments for further understanding the molecular mechanism of chemotaxis. It could be argued that the PI3K pathway is dispensable for chemotaxis and that PIP_3 is not required for chemotaxis. However, in wild-type cells, PIP_3 is formed at the leading edge in a cAMP gradient, and PIP_3 has pronounced effects on the time and place of pseudopod formation, suggesting that in wild-type cells, pseudopodia are always extended at places with elevated PIP_3 levels. Experiments investigating the role of PIP_3 in chemotaxis can be designed better now that we know that in PLA2-inhibited cells, chemotaxis fully depends on PI3K signaling. The same arguments can be used for the PLA2 pathway: it is dispensable for chemotaxis but functional in wild-type cells and can be investigated more specifically in *pi3k*-null cells. The notion that *D. discoideum* cells exhibit very good chemotaxis when either the PI3K or PLA2 pathway is inhibited implies that these pathways are not essential components of the cells' compass, suggesting that the compass is upstream of PI3K and PLA2. The compass might be identified by searching for molecules that are localized toward the pipette in cells with complete inhibition of PI3K and PLA2 signaling, and therefore also of all downstream components. The notion that all chemotaxis in *D. discoideum* is mediated by either PI3K or by PLA2 signaling provides a strong focus to unravel the obviously complex signaling cascades to actin polymerization and pseudopod formation at the leading edge in *D. discoideum*.

Materials and methods

Strains and growth conditions

The *D. discoideum* strain AX3 was used as wild-type control in all experiments. The mutants strains used are the *plc*-null strain 1.19 (Drayer et al., 1995), the *pi3k*-null *pi3k1*$^{-}$/*pi3k2*$^{-}$ strain GMP1 (Funamoto et al., 2001), and the *iplA*-null strain HM1038, lacking the IP_3 receptor (Traynor et al., 2000). Cells were grown in shaking culture in HG5 medium (contains, per liter, 14.3 g oxoid peptone, 7.15 g bacto yeast extract, 1.36 g $Na_2HPO_4 \times 12\ H_2O$, 0.49 g KH_2PO_4, and 10.0 g glucose) at a density between 5×10^5 and 6×10^6 cells/ml. Cells were harvested by centrifugation for 3 min at 300 *g*, washed in PB (10 mM KH_2PO_4/Na_2HPO_4, pH 6.5), and starved in PB in 6-well plates (Nunc) for 5 h. Cells were then resuspended in PB, centrifuged, washed once in PB, and resuspended in PB at a density of 6×10^6 cells/ml.

Chemotaxis

Chemotaxis measured with the small population assay (Konijn, 1970) was performed in the wells of a 6-well plate with 1 ml agar nonnutrient hydrophobic agar (11 mM KH_2PO_4, 2.8 mM Na_2HPO_4, and 7 g/liter hydrophobic agar) containing the indicated concentration of the drugs. Droplets of ~0.1 μl of 5 h–starved cells (6×10^6 cells/ml) were placed on the agar. After 30 min, chemotaxis toward cAMP was tested by placing a second

0.1 μl droplet, with the indicated concentration of cAMP, next to the droplet of cells. The distribution of the cells in the droplet was observed about every 10 min for 90 min. Chemotaxis of cells within a droplet was scored positive when the cell density at the cAMP side was at least twice as high as the opposite side of the droplet (Konijn, 1970). The maximal chemotactic response is faster for 50 nM cAMP (20–40 min) than for 1,000 nM cAMP (40–60 min). Also, some mutants respond faster (*plc*-null) or slower (*pi3k*-null) than wild-type cells. Recorded is the fraction of droplets scored positive, averaged over three successive observations at and around the moment of the maximal response. The data presented are the means and SEMs of at least three independent measurements on different days. Chemotaxis was also measured with micropipettes containing 100 μM cAMP using an inverted light microscope (CK40; Olympus) with a 20× NA 0.4 objective (LWD A240; Olympus) equipped with a charge-coupled device camera (TK-C1381; JVC). The field of observation is 358 × 269 μm. Images were captured every 10 s for 30 min on a PC using VirtualDub software and Indeo Video 5.10 (Ligos) compression. The chemotaxis index, defined as the ratio of the cell displacement in the direction of the gradient and its total traveled distance, was determined for ∼25 cells in a video as follows. First, the position of the centroid of a cell was determined with ImageJ (rsb.info.nih.gov/ij) for frames at 60-s intervals, yielding a series of coordinates for that cell. Using these coordinates, the chemotaxis index of each 60-s step was calculated and averaged, yielding the chemotaxis index for that cell in the video. The data shown are the mean and SEM of the chemotaxis indices from at least three independent experiments with ∼25 cells per experiment.

The same experimental setup with micropipettes was used for analyses of cells expressing the PIP_3 sensor PHcrac-GFP. Confocal images were recorded with a confocal laser-scanning microscope (LSM 510 META-NLO; Carl Zeiss MicroImaging, Inc.) equipped with a plan-apochromatic 63× NA 1.4 objective (Carl Zeiss MicroImaging, Inc.). For excitation of the fluorochrome GFP (S65T variant) a 488-nm argon/krypton laser was used, and the fluorescence was filtered through BP500-530 and IR LP560 and detected by a photomultiplier tube. The field of observation was 206 × 206 μm.

Gradients of cAMP during chemotavxis

In the small population assay, the applied cAMP diffuses in the agar, leading to a transient cAMP gradient at the cells. The maximal cAMP concentration *C(x)* and the absolute spatial gradient $\nabla C(x)$ are described as

$$C(x) = 0.48\frac{r^3}{x^3}C_d \text{ and } \nabla C(x) = 2.42\frac{r^3}{x^4}C_d,$$

where *r* is the radius of the cAMP droplet (150 μm), *x* is the distance between cell population and cAMP source (250 μm), and C_d is the applied cAMP concentration in the droplet. The absolute cAMP gradients at 50 and 1,000 nM cAMP are ∼100 and 2,000 pM/μm, respectively.

When a pipette filled with cAMP is inserted in a field of *D. discoideum* cells, cAMP will diffuse continuously from the pipette, leading within 1 min to a stable spatial gradient. The concentration *C(x)* and the spatial gradient $\nabla C(x)$ are dependent on the distance (*x*) from the pipette according to

$$C(x) = \alpha C_p / x \text{ and } \nabla C(x) = -\alpha C_p / x^2,$$

where C_p is the cAMP concentration in the pipette and α is a proportionality constant that depends on the geometry of the pipette and the applied pressure. The formation of the cAMP gradient was deduced by measuring the release of the fluorescent dye Lucifer yellow (mol wt = 457 D) from the pipette with the confocal fluorescent microscope and calibrated using the fluorescence intensity of diluted Lucifer yellow added homogeneously to the bath. The experiments yield $\alpha = 0.05$ and demonstrate that the equations are accurate descriptions of the cAMP gradient at a distance >15 μm from the pipette; at shorter distances, more complex equations are required. At 100, 50, and 20 μm from the pipette, the absolute cAMP gradient is 500, 2,000, and 12,500 pM/μm, respectively.

Online supplemental material

Table S1 presents the chemotaxis data obtained with the small population assay of ∼70 conditions with different combinations of cell strains and inhibitors. Video 1 shows chemotaxis of wild-type AX3 cells toward a pipette with cAMP in buffer. The PLA2 inhibitor BPB is added at 4 min, and the PI3K inhibitor LY294002 is added at 12 min. Video 2 shows the localization of PHcrac-GFP (detecting PIP_3) at the leading edge of wild-type cells chemotaxing toward cAMP. Video 3 shows *plc*-null cell movement toward a pipette with cAMP. Online supplemental material is available at http://www.jcb.org/cgi/content/full/jcb.200701134/DC1.

The mutant strains used in this study were obtained from the *Dictyostelium* stock center.

This research was supported by the Netherlands Organisation for Scientific Research.

Submitted: 25 January 2007
Accepted: 1 May 2007

References

Affolter, M., and C.J. Weijer. 2005. Signaling to cytoskeletal dynamics during chemotaxis. *Dev. Cell.* 9:19–34.

Baggiolini, M. 1998. Chemokines and leukocyte traffic. *Nature.* 392:565–568.

Bosgraaf, L., and P.J. van Haastert. 2006. The regulation of myosin II in *Dictyostelium*. *Eur. J. Cell Biol.* 85:969–979.

Campbell, J.J., and E.C. Butcher. 2000. Chemokines in tissue-specific and microenvironment-specific lymphocyte homing. *Curr. Opin. Immunol.* 12:336–341.

Chakraborti, S. 2003. Phospholipase A(2) isoforms: a perspective. *Cell. Signal.* 15:637–665.

Chen, L., M. Iijima, M. Tang, M.A. Landree, Y.E. Huang, Y. Xiong, P.A. Iglesias, and P.N. Devreotes. 2007. PLA2 and PI3K/PTEN pathways act in parallel to mediate chemotaxis. *Dev. Cell.* 12:603–614.

Crone, S.A., and K.F. Lee. 2002. The bound leading the bound: target-derived receptors act as guidance cues. *Neuron.* 36:333–335.

Drayer, A.L., J. van der Kaay, G.W. Mayr, and P.J.M. van Haastert. 1994. Role of phospholipase C in *Dictyostelium*: formation of inositol 1,4,5-trisphosphate and normal development in cells lacking phospholipase C activity. *EMBO J.* 13:1601–1609.

Drayer, A.L., M.E. Meima, M.W.M. Derks, R. Tuik, and P.J.M. van Haastert. 1995. Mutation of an EF-hand Ca^{2+}-binding motif in phospholipase C of *Dictyostelium discoideum*: inhibition of activity but no effect on Ca^{2+}-dependence. *Biochem. J.* 311:505–510.

Franca-Koh, J., Y. Kamimura, and P.N. Devreotes. 2007. Leading-edge research: PtdIns(3,4,5)P(3) and directed migration. *Nat. Cell Biol.* 9:15–17.

Funamoto, S., K. Milan, R. Meili, and R.A. Firtel. 2001. Role of phosphatidylinositol 3′ kinase and a downstream pleckstrin homology domain-containing protein in controlling chemotaxis in *Dictyostelium*. *J. Cell Biol.* 153:795–809.

Funamoto, S., R. Meili, S. Lee, L. Parry, and R.A. Firtel. 2002. Spatial and temporal regulation of 3-phosphoinositides by PI 3-kinase and PTEN mediates chemotaxis. *Cell.* 109:611–623.

Hirsch, E., V.L. Katanaev, C. Garlanda, O. Azzolino, L. Pirola, L. Silengo, S. Sozzani, A. Mantovani, F. Altruda, and M.P. Wymann. 2000. Central role for G protein-coupled phosphoinositide 3-kinase gamma in inflammation. *Science.* 287:1049–1053.

Huang, Y.E., M. Iijima, C.A. Parent, S. Funamoto, R.A. Firtel, and P.N. Devreotes. 2003. Receptor mediated regulation of PI3Ks confines PI(3,4,5)P3 to the leading edge of chemotaxing cells. *Mol. Biol. Cell.* 14:1913–1922.

Iijima, M., and P. Devreotes. 2002. Tumor suppressor PTEN mediates sensing of chemoattractant gradients. *Cell.* 109:599–610.

Iijima, M., Y.E. Huang, H.R. Luo, F. Vazquez, and P.N. Devreotes. 2004. Novel mechanism of PTEN regulation by its phosphatidylinositol 4,5-bisphosphate binding motif is critical for chemotaxis. *J. Biol. Chem.* 279:16603–16613.

Konijn, T.M. 1970. Microbiological assay for cyclic 3′,5′-AMP. *Experientia.* 26:367–369.

Loovers, H.M., M. Postma, I. Keizer-Gunnink, Y.E. Huang, P.N. Devreotes, and P.J. van Haastert. 2006. Distinct roles of PI(3,4,5)P3 during chemoattractant signaling in *Dictyostelium*: a quantitative in vivo analysis by inhibition of PI3-kinase. *Mol. Biol. Cell.* 17:1503–1513.

Parent, C.A., B.J. Blacklock, W.M. Froehlich, D.B. Murphy, and P.N. Devreotes. 1998. G protein signaling events are activated at the leading edge of chemotactic cells. *Cell.* 95:81–91.

Postma, M., L. Bosgraaf, H.M. Loovers, and P.J.M. Van Haastert. 2004a. Chemotaxis: signalling modules join hands at front and tail. *EMBO Rep.* 5:35–40.

Postma, M., J. Roelofs, J. Goedhart, H.M. Loovers, A.J.W.G. Visser, and P.J.M. Van Haastert. 2004b. Sensitisation of *Dictyostelium* chemotaxis by PI3-kinase mediated self-organising signalling patches. *J. Cell Sci.* 117:2925–2935.

Seastone, D.J., L.Y. Zhang, G. Buczynski, P. Rebstein, G. Weeks, G. Spiegelman, and J. Cardelli. 1999. The small Mr Ras-like GTPase Rap1 and the phospholipase C pathway act to regulate phagocytosis in *Dictyostelium discoideum*. *Mol. Biol. Cell.* 10:393–406.

Servant, G., O.D. Weiner, P. Herzmark, T. Balla, J.W. Sedat, and H.R. Bourne. 2000. Polarization of chemoattractant receptor signaling during neutrophil chemotaxis. *Science.* 287:1037–1040.

Traynor, D., J.L.S. Milne, R.H. Insall, and R.R. Kay. 2000. Ca^{2+} signalling is not required for chemotaxis in *Dictyostelium*. *EMBO J.* 19:4846–4854.

Tsaneva-Atanasova, K., D.I. Yule, and J. Sneyd. 2005. Calcium oscillations in a triplet of pancreatic acinar cells. *Biophys. J.* 88:1535–1551.

van Dijken, P., J.R. de Haas, A. Craxton, C. Erneux, S.B. Shears, and P.J.M. van Haastert. 1995. A novel, phospholipase C-independent pathway of inositol1, 4,5-trisphosphate formation in *Dictyostelium* and rat liver. *J. Biol. Chem.* 270:29724–29731.

Van Haastert, P.J.M., and P.N. Devreotes. 2004. Chemotaxis: signalling the way forward. *Nat. Rev. Mol. Cell Biol.* 5:626–634.

Wang, F., P. Herzmark, O.D. Weiner, S. Srinivasan, G. Servant, and H.R. Bourne. 2002. Lipid products of PI(3)Ks maintain persistent cell polarity and directed motility in neutrophils. *Nat. Cell Biol.* 4:513–518.

Ward, S.G. 2004. Do phosphoinositide 3-kinases direct lymphocyte navigation? *Trends Immunol.* 25:67–74.

Ward, S.G. 2006. T lymphocytes on the move: chemokines, PI 3-kinase and beyond. *Trends Immunol.* 27:80–87.

Xu, J., F. Wang, A. Van Keymeulen, P. Herzmark, A. Straight, K. Kelly, Y. Takuwa, N. Sugimoto, T. Mitchison, and H.R. Bourne. 2003. Divergent signals and cytoskeletal assemblies regulate self-organizing polarity in neutrophils. *Cell.* 114:201–214.